

Potential Energy Surface of 1,6-Methano[10]annulen-11-ylidene and Its Isomers

David A. Modarelli

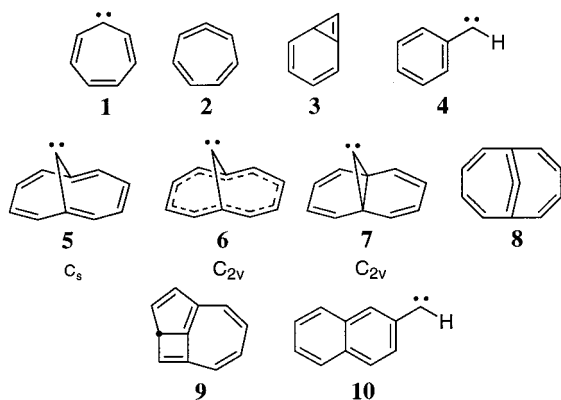
Department of Chemistry, Knight Chemical Laboratory, The University of Akron, Akron, Ohio 44325-3601

dam@chemistry.uakron.edu

Received February 9, 2000 (Revised Manuscript Received July 12, 2000)

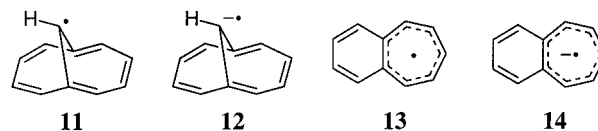
The potential energy surface of 1,6-methano[10]annulen-11-ylidene and its isomers has been investigated by density functional (BLYP and B3LYP) molecular orbital methods. These calculations indicate the lowest energy annulene structure to be 56.9 kcal mol⁻¹ higher in energy than triplet 1-naphthylcarbene. These calculations, together with calculations on transition states connecting possible rearrangement products derived from this carbene, indicate that the trapping products reported by Carlton et al. *J. Am. Chem. Soc.* **1976**, *98*, 6068–6070 arise from rearrangement of the annulene–carbene to a tricyclic isomer.

Carbene rearrangements have long fascinated physical organic chemists. Recent theoretical results^{1–3} investigating the potential energy surface (PES), the spectroscopy and rearrangements of the cycloheptatrienylydene (**1**)/cycloheptatetraene (**2**)/bicyclo[4.1.0]hepta-2,4,6-triene (**3**)/phenylcarbene (**4**) tetrad, and the related rearrangements in the naphthylcarbene series⁴ prompted us to examine the stability of 1,6-methano[10]annulen-11-ylidene (**5**) and its isomers (**6–10**).



The only experimental work attempting to generate and trap **5** was done by Carlton et al.,⁵ who reacted 11,11-dichlorotricyclo[4.4.1.0^{1,6}]undecane with methyl-lithium. Product analysis showed the formation of an unstable and unidentified dimer. Trapping studies with 1,3-diphenylisobenzofuran (DPIBF) indicated the only trappable species to be either allene **8** or its electrocyclic ring-closure product, **9**. Direct observations using matrix isolation or time-resolved techniques have not been reported on **5–8**, largely because of a lack of a suitable precursor for carbene generation by flash vacuum pyrolysis or photochemical methods.

Carbene **1** is structurally quite different from **5/6**, where the bridging carbons at C₁ and C₆ in **5/6** force the carbene carbon to be symmetrically disposed with regard to the annulene ring and prevent any stabilization due to conjugation. However, rearrangements of the related radicals (**11**) and radical ions (**12**) yield products (**13** and **14**)⁶ that are analogous to the **1–4** interconversion. Chapman, McMahon, and others⁷ have demonstrated experimentally that the PES of the naphthylcarbenes is quite complex. Recent calculations by Xie et al.⁴ have clarified the PES for these molecules considerably. Thus, although there are considerable structural differences between **1** and **5**, the possibility of such rearrangements suggested that calculations on an isomer such as **10** are necessary to benchmark the relative stabilities of **5–8**, even though they were not trapped by Levin and co-workers.



Carbene **5** is also interesting as a model for buckminsterfullerenylidene (C₆₁; Figure 1),⁸ which is a molecule that has interesting applications in the synthesis of novel materials. Because of its large size, current computational limitations prohibit accurate predictions of the structure and resulting spin state of such a molecule.

The bonding at the C₁ and C₆ bridging carbon atoms on carbenes **5–7** and allene **8** presents an interesting

(6) Gerson, F.; Huber, W.; Müllen, K. *Helv. Chim. Acta* **1979**, *62*, 2109.

(7) Albrecht, S. W.; McMahon, R. J. *J. Am. Chem. Soc.* **1993**, *115*, 855–859. West, P. R.; Mooring, A. M.; McMahon, R. J.; Chapman, O. L. *J. Org. Chem.* **1986**, *51*, 1316–1320. See also the following: Jones, W. M.; Ennis, C. L. *J. Am. Chem. Soc.* **1969**, *91*, 6391. West, P. R.; Chapman, O. L.; LeRoux, J.-P. *J. Am. Chem. Soc.* **1982**, *104*, 1779. McMahon, R. J.; Chapman, O. L. *J. Am. Chem. Soc.* **1986**, *108*, 1713. Kuzaj, M.; Lüerssen, H.; Wentrup, C. *Angew. Chem., Int. Ed. Engl.* **1986**, *25*, 480. Engler, T. A.; Shechter, H. *Tetrahedron Lett.* **1982**, *23*, 2715. West, P. R.; Mooring, A. M.; McMahon, R. J.; Chapman, O. L. *J. Org. Chem.* **1986**, *51*, 1316. Chapman, O. L.; Sheridan, R. S.; LeRoux, J.-P. *Recl. Trav. Chim. Pays-Bas* **1979**, *98*, 334. Barcus, R. L.; Hadel, L. M.; Johnston, L. J.; Platz, M. S.; Savino, T. G.; Scaiano, J. C. *J. Am. Chem. Soc.* **1986**, *108*, 3928. Horn, K. A.; Chateaufneuf, J. E. *Tetrahedron* **1985**, *41*, 1465. Jones, W. M. In *Rearrangements in Ground and Excited States*; DeMayo, P., Ed.; Academic Press: New York, 1980; Vol. 1, Chapter 3.

(1) Matzinger, S.; Bally, T.; Patterson, E. V.; McMahon, R. J. *J. Am. Chem. Soc.* **1996**, *118*, 1535–1542.

(2) Schreiner, P. R.; Karney, W. L.; von R. Schleyer, P.; Borden, W. T.; Hamilton, T. P.; Schaefer, H. F., III. *J. Org. Chem.* **1996**, *61*, 7030–7039.

(3) Wong, M. W.; Wentrup, C. *J. Org. Chem.* **1996**, *61*, 7022–7029.

(4) Xie, Y.; Schreiner, P. R.; Schleyer, P. V. R.; Schaefer, H. F. *J. Am. Chem. Soc.* **1997**, *119*, 1370–1377.

(5) Carlton, J. B.; Levin, R. H.; Clardy, J. *J. Am. Chem. Soc.* **1976**, *98*, 6068–6070.

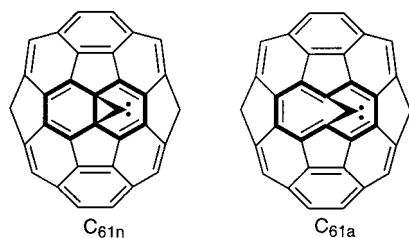


Figure 1. Buckminsterfullerenylidene shown in two potential forms, in the tricyclic norcaradiene form (C_{61n}) and in the bicyclic annulene form (C_{61a}). The analogous compounds we have chosen to model are shown with bold lines.

variety of destabilizing structural forces.⁹ These bridge-head carbons force the carbene carbon to be either slightly tilted to one side (C_s symmetry; **5**) or normal to the annulene ring (C_{2v} symmetry; **6**). In either case, the π and σ orbitals on the carbene carbon cannot interact by conjugation with the aromatic ring. Carbene **7** possesses a large amount of ring strain, although hyperconjugation of the empty p orbital in the singlet carbene with the sp^2 -hybridized Walsh σ -type orbitals on the cyclopropyl ring is possible. Finally, allene **8** is expected to be quite strained, and the cumulative bond is likely twisted. In this paper, we report a density functional theory (DFT) computational study of **5** and its isomers (carbenes **6** and **7**, allene **8**, and the possible rearrangement products **9** and **10**) and the PES leading from carbene **5** (or **6**) to the trapped intermediate observed by Levin.

Computational Methodology

Geometry optimizations were performed at the Hartree-Fock level as well as using Becke's gradient-corrected (original¹⁰ and three-parameter¹¹) exchange functionals with the correlation functional of Lee et al.¹² (BLYP and B3LYP, respectively¹³). Single-point energies were computed at both the B3LYP/TZP and BLYP/TZP levels with Dunning's correlation consistent triple- ζ basis set (cc-pVTZ)¹⁴ and the B3LYP/6-31G(d)- and BLYP/6-31G(d)-optimized geometries, respectively. When used with the 6-31G(d) basis set, the DFT functionals¹³ have been shown to give excellent agreement with both the experiment⁴ and higher levels of theory.^{1,2} Because of the relatively large size of **5**, calculations including dynamic correlation were not performed (i.e., a CASPT2N calculation would require a 12 orbital/12 electron (12/12) active

space to include all π electrons). Schreiner et al.² have indicated that inclusion of dynamic correlation (CASPT2N and CCSD) is more important for delocalized systems such as **10** rather than **5–9**. Because we were primarily interested in the energies of **5–9** relative to one another, and not to the much more stable rearrangement products (i.e., **10**), we decided calculations including dynamic correlation were not necessary at this time. In any case, DFT methods recover some electron correlation. Results obtained using the DFT methods¹ have also been shown to agree qualitatively with higher level CCSD(T) and CASPT2N² calculations and often give better results than the G2 (SVP and MP2) level.³ It should be noted that density functional methods are known to overstabilize allene energies somewhat.¹⁵

Vibrational analysis was performed using second analytical derivatives for all optimized structures. Transition-state structures were located using the Synchronous Transit-Guided Quasi-Newton method developed by Peng and Schlegel¹⁶ and were performed at the B3LYP/6-31G(d) and BLYP/6-31G(d) levels. IRC calculations were performed at the B3LYP/6-31G(d) level. All calculations were performed with the *Gaussian 94*¹⁷ and *Gaussian 98*¹⁸ sets of programs. Molecular orbitals were visualized using MacMolPlt¹⁹ and calculated with MacGAMESS.²⁰ Imaginary vibrations were observed using an animation program.

Results and Discussion

The absolute and relative energies of carbenes **5**, **6**, and **10**, allene **8**, and its rearrangement product, **9**, are shown in Table 1. The relative energies of **5–10** calculated at the B3LYP/TZP//B3LYP/6-31G(d) and BLYP/TZP//BLYP/6-31G(d) levels are shown in Figure 2. The results obtained at the B3LYP/TZP//B3LYP/6-31G(d) level will be referred to in the text. Consistent with both the experiment^{7,21} and Schaefer's calculations, triplet 2-naphthylcarbene (**10T**) is the most stable isomer examined upon the PES at all levels of theory considered except

(15) Houk, K. N.; Plattner, D. A. *J. Am. Chem. Soc.* **1995**, *117*, 4405.

(16) Peng, C.; Schlegel, H. B. *Isr. J. Chem.* **1993**, *33*, 449.

(17) Frisch, M. J.; Trucks, G. W.; Schlegel, H. B.; Gill, P. M. W.; Johnson, B. G.; Robb, M. A.; Cheeseman, J. R.; Keith, T.; Petersson, G. A.; Montgomery, J. A.; Raghavachari, K.; Al-Laham, M. A.; Zakrzewski, V. G.; Ortiz, J. V.; Foresman, J. B.; Cioslowski, J.; Stefanov, B. B.; Nanayakkara, A.; Challacombe, M.; Peng, C. Y.; Ayala, P. Y.; Chen, W.; Wong, M. W.; Andres, J. L.; Replogle, E. S.; Gomperts, R.; Martin, R. L.; Fox, D. J.; Binkley, J. S.; Defrees, D. J.; Baker, J.; Stewart, J. P.; Head-Gordon, M.; Gonzalez, C.; Pople, J. A. *Gaussian 94*, Rev. E.2; Gaussian, Inc.: Pittsburgh, PA, 1995.

(18) Frisch, M. J.; Trucks, G. W.; Schlegel, H. B.; Scuseria, G. E.; Robb, M. A.; Cheeseman, J. R.; Zakrzewski, V. G.; Montgomery, J. A., Jr.; Stratmann, R. E.; Burant, J. C.; Dapprich, S.; Millam, J. M.; Daniels, A. D.; Kudin, K. N.; Strain, M. C.; Farkas, O.; Tomasi, J.; Barone, V.; Cossi, M.; Cammi, R.; Mennucci, B.; Pomelli, C.; Adamo, C.; Clifford, S.; Ochterski, J.; Petersson, G. A.; Ayala, P. Y.; Cui, Q.; Morokuma, K.; Malick, D. K.; Rabuck, A. D.; Raghavachari, K.; Foresman, J. B.; Cioslowski, J.; Ortiz, J. V.; Stefanov, B. B.; Liu, G.; Liashenko, A.; Piskorz, P.; Komaromi, I.; Gomperts, R.; Martin, R. L.; Fox, D. J.; Keith, T.; Al-Laham, M. A.; Peng, C. Y.; Nanayakkara, A.; Gonzalez, C.; Challacombe, M.; Gill, P. M. W.; Johnson, B.; Chen, W.; Wong, M. W.; Andres, J. L.; Gonzalez, C.; Head-Gordon, M.; Replogle, E. S.; Pople, J. A. *Gaussian 98*, Rev. A.6; Gaussian, Inc.: Pittsburgh, PA, 1998.

(19) Bode, B. M.; Gordon, M. S. *J. Mol. Graphics Modell.* **1998**, *16*, 133.

(20) Schmidt, M. W.; Baldrige, K. K.; Boatz, J. A.; Elbert, S. T.; Gordon, M. S.; Jensen, J. H.; Koseki, S.; Matsunaga, N.; Nguyen, K. A.; Su, S. J.; Windus, T. L.; Dupuis, M.; Montgomery, J. A. *J. Comput. Chem.* **1993**, *14*, 1347.

(21) Trozzolo, A. M.; Wasserman, E.; Yager, W. A. *J. Am. Chem. Soc.* **1965**, *87*, 129.

(8) See, for example, the following: Slanina, Z.; Lee, S. L. *THEOCHEM* **1994**, *110*, 173–179. Christian, J. F.; Wan, Z.; Anderson, S. L. *J. Phys. Chem.* **1992**, *96*, 3574–3576. Cui, Y.; Liu, L. *Phys. Rev. B: Condens. Matter* **1997**, *56*, 3624–3627.

(9) The parent hydrocarbon has received considerable experimental and theoretical treatment over the past decade because of its important implications regarding the function of orbital overlap in aromaticity and its unusual bonding at the bridging carbons C_1 and C_6 ; see, for example, the following references: Sironi, M.; Raimondi, M.; Cooper, D. L.; Gerratt, J. *J. Mol. Struct.: THEOCHEM* **1995**, *338*, 257–265. Haddon, R. C.; Raghavachari, K. *J. Am. Chem. Soc.* **1985**, *107*, 289–298. Farnell, L.; Radom, L. *J. Am. Chem. Soc.* **1982**, *104*, 7650–7654. Frydman, L.; Frydman, B.; Kustanovich, I.; Vega, S.; Vogel, E.; Yannoni, C. *J. Am. Chem. Soc.* **1990**, *112*, 6472–6476.

(10) Becke, A. D. *Phys. Rev. A: At., Mol., Opt. Phys.* **1988**, *38*, 3098.

(11) Becke, A. D. *J. Chem. Phys.* **1993**, *98*, 5648.

(12) Lee, C.; Yang, W.; Parr, R. G. *Phys. Rev. B: Condens. Matter* **1988**, *37*, 785.

(13) A description of the Gaussian implementation of density functionals can be found in the following: Johnson, B. G.; Gill, P. M. W. L.; Pople, J. A. *J. Chem. Phys.* **1993**, *98*, 5612.

(14) Kendall, R. A.; Dunning, T. H., Jr.; Harrison, R. J. *J. Chem. Phys.* **1992**, *96*, 6796.

Table 1. Relative Energies (in kcal mol⁻¹) of C₁₁H₈ Isomers by Different Quantum Chemical Methods^a

structure	point group	HF/6-31G(d)	BLYP/6-31G(d)	BLYP/TZP//		B3LYP/TZP//		B3LYP/TZP//
				BLYP/6-31G(d)	B3LYP/6-31G(d)	B3LYP/6-31G(d)	B3LYP/6-31G(d) + ZPVE	
5T	C _s	-17.7 (1)	0.8 (0)	2.7	-0.9 (0)	1.4	2.5	
5S	C _s	0.0 (0)	0.0 (0)	0.0	0.0 (0)	0.0	0.0	
6S	C _{2v}	1.8 (1)	0.4 (1)	0.1	0.2 (1)	0.0	-0.4	
6T	C _{2v}	-14.8 (1)	0.8 (0)	2.7	-0.9 (0)	1.4	2.5	
7S	C _{2v}	-0.8 (1)						
7T	C _{2v}							
8	C ₂	15.7 (0)	4.7 (0)	5.1	6.2 (0)	6.9	7.7	
9	C ₁	-29.9 (0)	-28.6 (0)	-26.0	-31.4 (0)	-28.8	-26.7	
10S	C _s	-66.9 (0)	-47.7 (0)		-52.3 (0)	-51.2	-49.8	
10T	C _s	-30.5 (0)	-53.1 (0)	-51.0	-59.2 (0)	-56.9	-55.9	
15	C ₁	-51.5 (0)	-57.3 (0)	-55.9	-57.3 (0)	-55.8	-53.8	
TS1	C ₁		12.6 (1)	13.7	17.9 (1)	16.5	16.5	
TS3	C ₁		3.5 (1)	4.0	4.5 (1)	5.1	5.2	
TS4	C ₁		19.8 (1)	22.6	20.4 (1)	23.1	24.0	

^a The number in parentheses denotes the number of imaginary frequencies. ^b Calculation results in ring opening across the C₁-C₆ bond to yield structure **6S**. ^c This calculation did not yield a stable structure but resulted instead in the formation of naphthalene and a carbon atom. ^d Wave function did not converge. ^e Not determined.

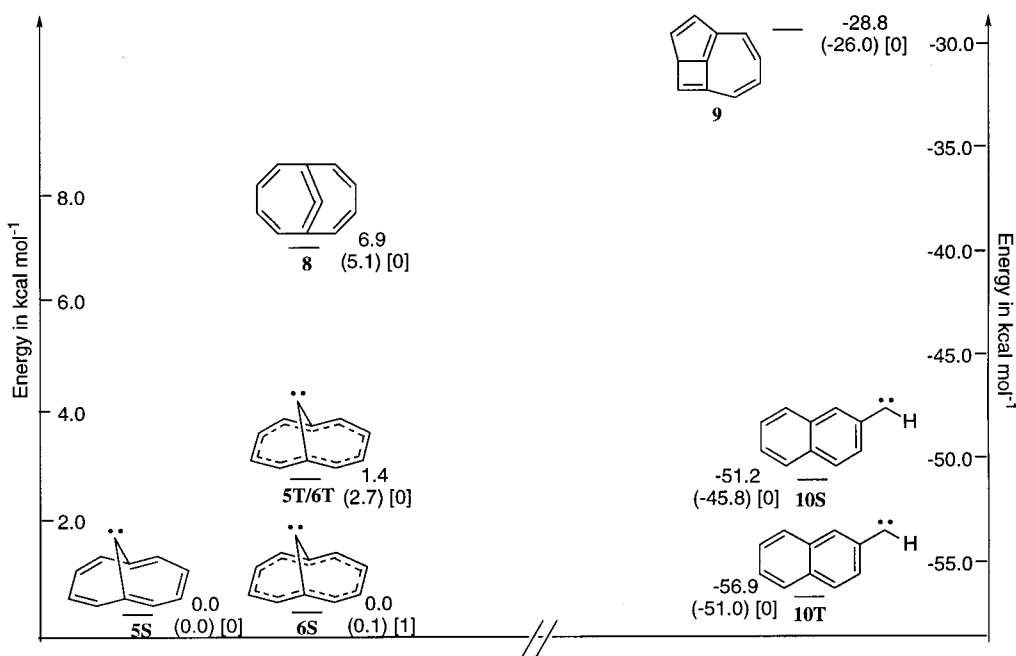


Figure 2. Schematic representation of the relative energies of the C₁₁H₈ isomers and electronic states considered in the present work. Energies are listed for the B3LYP/TZP/B3LYP/6-31G(d) and BLYP/TZP//BLYP/6-31G(d) levels of theory, and the number of imaginary frequencies is shown in brackets. Note that the scales for the annulenic carbenes at the left of the figure are different than those on the right and that the lowest energy annulene carbene **5S** is 56.9 kcal mol⁻¹ higher in energy than **10T**.

Hartree-Fock, where singlet 2-naphthylcarbene (**10S**) is lower in energy. Slightly higher in energy at the DFT levels is **10S** by 5.7 kcal mol⁻¹ (B3LYP/TZP). Substantially higher in energy are **5**-**9**. The tricyclic rearrangement product (**9**) is the lowest energy isomer of this series, ~28 kcal mol⁻¹ higher in energy than **10T**. Singlet carbene **5S**, having C_s symmetry and representing the localized annulene geometry, is the lowest energy annulene isomer, 56.9 kcal mol⁻¹ higher than **10T**. The delocalized singlet (**6S**), having C_{2v} symmetry, was found at all levels of theory to correspond to a transition state, with its imaginary vibration (-174i cm⁻¹) corresponding to the bond alternation of **5S**. Because of the small energetic differences between these isomers ($\Delta E_{6S-5S} \sim 0$ kcal mol⁻¹), we surmise that a small double minimum exists on the PES where **5S** and **6S** are virtually indistinguishable from one another. Triplet **5T** and **6T** are both minima, nearly structurally equivalent, and only 1.4 kcal mol⁻¹ higher in energy than **5S** at the B3LYP/

TZP level (+58.2 kcal mol⁻¹ higher than **10T**). The highest energy structure that is a minimum on the PES is allene **8**, which is 6.9 kcal mol⁻¹ higher in energy than **5T** and 63.7 kcal mol⁻¹ higher than **10T**. This general ordering is consistent for all density functional levels of theory considered here except B3LYP/6-31G(d) where the **5S/5T** order reverses. Calculations using input structures corresponding to norcaradiene (**7S**) were found at all levels of theory to optimize to **6S**. Triplet **7T** dissociates to a carbon atom and naphthalene at all levels.

The geometries of **5**, **8**, and **9** are shown in Figures 3 and 4. Carbene **6S** is a transition state, whereas **6T** is nearly identical in structure and energy to **5T**; so, neither is shown. Nonpertinent bond lengths and angles can be obtained from the Supporting Information. Certain relevant structural features will be discussed here.

The carbene bond angle (C₁-C₁₁-C₆) of **5S** is normal for singlet carbenes at 102° (B3LYP/6-31G(d)). This angle results in a C₁-C₆ distance of 2.282 Å, that is, 0.025 Å

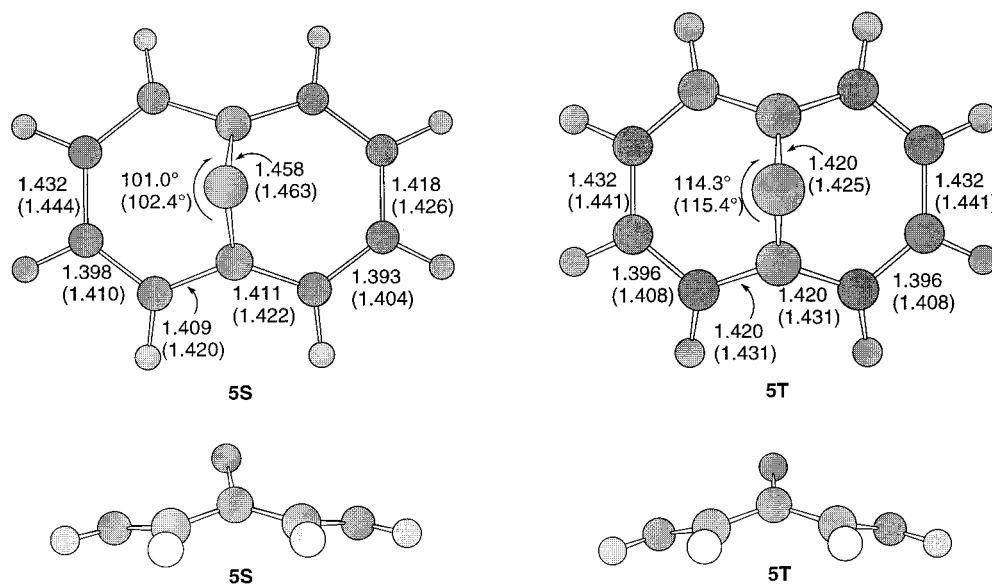


Figure 3. Bond lengths and $C_1-C_{11}-C_6$ bond angle for carbenes **5S** and **5T**. The values given were calculated at the B3LYP/6-31G(d) and BLYP/6-31G(d) levels. Bond lengths are given in angstroms and are indicated in the figure by full arrows; bond angles are indicated using half-arrows.

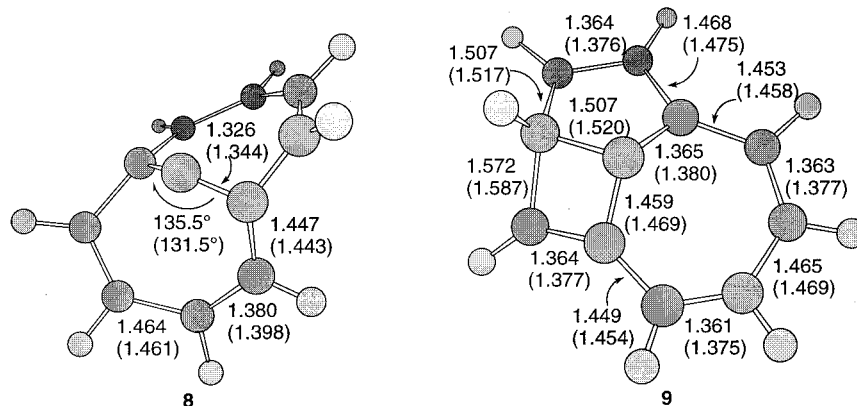


Figure 4. Bond lengths and $C_1-C_{11}-C_6$ bond angle for allene **8** and the tricyclic molecule **9**. The values given were calculated at the B3LYP/6-31G(d) and BLYP/6-31G(d) levels. Bond lengths are given in angstroms and are indicated in the figure by full arrows; bond angles are indicated using half-arrows.

longer than the parent hydrocarbon (2.257 Å found by electron diffraction;²² calculations at the HF/6-31G(d) level on the parent hydrocarbon indicate a distance for annulene of 2.263 Å with C_s symmetry and 2.246 Å with C_{2v} symmetry²³). The localized C_s geometry leads to the carbene carbon (C_{11}) tilting toward one side of the annulene ring. The $C_1-C_{11}-C_6$ angle for triplet **5T/6T** is larger than that of **5S/6S** at 115° (B3LYP/6-31G(d)) and has a C_1-C_6 distance of 2.410 Å. The increased bond angle in the triplet leads to a substantial decrease in the C_1-C_6 and C_1-C_{11} distances (1.425 Å) relative to the singlet **5S** (1.463 Å).

Allene **8** optimizes into a C_2 geometry and as expected shows a large amount of twisting at the allenic carbon (C_{11} ; Figure 4), forming dihedral angles of 50 and 98° with the annulene ring. The C_1-C_{11} and C_6-C_{11} bond lengths of 1.326 Å (B3LYP/6-31G(d)) are slightly longer than the typical allene $C=C$ bond distance of ~ 1.31 Å²⁴ and reflect the increased strain of being part of a ring. The C_1-C_6

distance is 2.454 Å, and the $C_1-C_{11}-C_6$ bond angle in this molecule is nonlinear (135°). Inspection of the HOMO (Figure 5) indicates a bonding interaction between the p orbitals localized on carbons C_1 and C_6 (via the lobes endo to the molecule) with the π orbital localized on C_{11} . Calculations at the GVB/6-31G(d) level indicate that there is no diradical character to this molecule.

Spin-State Preferences of 1,6-Methano[10]annulene-11-ylidene. Of the annulene carbenes **5** and **6**, carbene **5S/6S** is found to be lower in energy than **5T/6T** by a small margin. However, these carbenes are close enough in energy to be considered nearly degenerate at the levels of theory considered in this study. Nonetheless, we can speculate on the factors that contribute toward stabilization and destabilization of the singlet state.

Bond angle–spin-state analyses can be used to predict spin-state multiplicity crudely.²⁵ Of the annulene carbenes **5–7**, singlet carbene **5S** is the lowest energy species at the theoretical levels considered here. The $C_1-C_{11}-C_6$ bond angle (102°) is very close to that of singlet

(22) Coetzer, J. *Diss. Abstr. B* **1969**, 29, 3671.

(23) Haddon, R. C.; Raghavachari, K. *J. Am. Chem. Soc.* **1985**, 107, 289.

(24) March, J. *Advanced Organic Chemistry*, 4th ed.; Wiley-Interscience: New York, 1992; p 21.

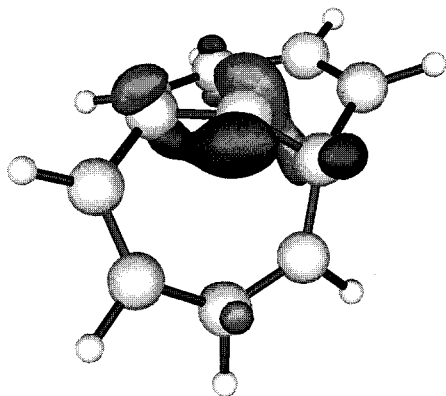


Figure 5. The HOMO of allene **8**.

methylene (102.4° for the 1A_1 singlet)²⁶ and singlet phenylcarbene ($\sim 107^\circ$)² and can be considered “normal” for singlet carbenes. Triplet **5T** has a $C_1-C_{11}-C_6$ angle of $\sim 115^\circ$. Such an angle is considerably smaller than that of triplet methylene (136° for the 3B_1 triplet)²⁶ or triplet phenylcarbene ($130-134.5^\circ$).² In the absence of other effects, it is clear that bond angle constriction in **5T** will raise the energy of the triplet state relative to **5S**.

The singlet state of **4** is stabilized relative to the corresponding singlet state, by resonance interaction of the electron in the π orbital with the aromatic ring.² Although annulene rings have aromatic character, the singly occupied π orbital in **5T** is orthogonal to the ring. Stabilization of the doubly occupied σ orbital in the singlet requires interaction with a low-lying unoccupied ring molecular orbital. An analysis of the molecular orbitals indicates that only the high-energy LUMO+3 orbital can interact with proper symmetry; therefore, the singlet state is not stabilized by the aromatic annulene ring. These carbenes therefore probably behave more like simple alkylcarbenes,²⁷ and stabilization due to the aromatic ring is not realized. The singlet may instead be destabilized by the symmetry-allowed interaction of this orbital with a ring molecular orbital of correct symmetry. Thus, bond angle effects favor the singlet spin state, while orbital interactions have the opposite effect and destabilize the singlet relative to the triplet.

Interpretation of Trapping Experiments. Carlton et al. were able to identify an adduct that was attributed to cycloaddition of either **8** (followed by electrocyclic ring closure) or **9** with DPIBF.⁵ No evidence was found in the product studies indicating formation of carbenes **5-7**, nor were products indicative of a rearrangement to the much more stable **10** or benzocycloheptatetraene (**15**) found. Trapping products from **5** were not detected in the product analysis despite the fact that **5** is more stable than **8** by nearly 8 kcal mol^{-1} . To address this seeming anomaly, we decided to examine the PES to determine the energetics of the conversion of **5** to **8** or **9**. In this way we hoped to determine the intermediate most likely trapped with DPIBF. Levin's crystallographic and NMR-

labeling data are consistent with trapping of either **8** or **9**, and so it seemed prudent to examine the transition states connecting both **5** \rightarrow **8** and **8** \rightarrow **9**, as well as the direct path **5** \rightarrow **9**.

At the B3LYP/TZP//B3LYP/6-31G(d) level of theory, the transition state connecting **5** with **8** (**TS1**, -389 cm^{-1} ; Figure 6) is $\sim 16.5 \text{ kcal mol}^{-1}$ higher than **5**. Such a barrier should result in a slow conversion of **5** to **8** under the experimental conditions used in Levin's work (-30°C). The side view of **TS1** shown in Figure 6 clearly demonstrates the significant flattening and twisting of the 10-membered ring in the transition state. The bond angle at $C_1-C_{11}-C_6$ increases in **TS1** to nearly 127° (from an angle of 101.0° for **5**), well on its way to the 135.5° found in the allene and consistent with a late transition state. We were unsuccessful in locating the second transition state on this path (**TS2**, connecting **8** and **9**) using Schlegel's QST2 and QST3 algorithms.

Calculations on the third transition state, that directly connects **5** and **9** (**TS3**; Figure 6), indicate a much smaller barrier height of $5.1 \text{ kcal mol}^{-1}$. Because of the exothermicity of the rearrangement ($-28.8 \text{ kcal mol}^{-1}$), it is not surprising to find an early transition state where **TS3** is structurally quite similar to the carbene (**5S**). Inspection of this transition state reveals carbon atoms C_{11} and C_3 bending toward one another to begin formation of the new single bond (see **TS3**, bottom drawing), and in the transition state they are 2.194 \AA away from one another (compared with distances of 2.670 \AA in **5** and 1.507 \AA in **9**). The interatomic distances in this structure are also consistent with an early transition state.

Levin et al. were unable to detect evidence of the formation of **15** by way of chemical trapping experiments. Nonetheless, the very exothermic reaction of **5** to **15**, formally a 1,2-C shift from one of the bridging carbons to the carbene carbon, indicates that formation of **15** should be possible. To determine the likelihood of this rearrangement, the transition state (**TS4**) connecting carbene **5S** to **15** was calculated at the B3LYP and BLYP density functional levels. Examination of this transition state (Figure 7) reveals substantial atomic reorganization. The migrating carbon atom (C_2) rotates, initiating bond formation of the p orbital formerly involved in a π bond with the empty p orbital at C_{11} , the carbene center. At this time, the unpaired electrons at C_{11} have also initiated π -bond formation with the former bridgehead carbon C_1 . The resulting electronic distribution is quite visible (Figure 7), where the formerly delocalized bonds have localized into double bonds between C_3-C_4 , C_5-C_6 , C_7-C_8 , and C_9-C_{10} . Interestingly, this process results in the carbene carbon atom attaining a nearly 180° angle with C_1 and C_6 . Such structural changes come at a significant cost: at the B3LYP/TZP level, **TS4** is calculated to be $23.1 \text{ kcal mol}^{-1}$ higher in energy than **5** (Table 1). Because of the high relative energy required to reach **TS4**, formation of **15** cannot compete with formation of **9**, which passes through **TS3** ($\Delta H^\ddagger \sim 5.1 \text{ kcal mol}^{-1}$). The thermodynamically favored product is therefore not formed.

On the basis of these calculations, we propose a PES as shown in Figure 8 to explain the experimentally observed trapping chemistry. The very exothermic rearrangement channel **5** \rightarrow **15** (and through **15**, 2-naphthylcarbene (**10**)⁴) is not observed experimentally. According to the proposed mechanism, formation of **5/6** is rapidly followed by rearrangement to **9** (and precluding

(25) Hoffman, R.; Zeiss, G. D.; Van Dine, G. W. *J. Am. Chem. Soc.* **1968**, *90*, 1485.

(26) Yamaguchi, Y.; Sherrill, C. D.; Schaefer, H. F., III. *J. Phys. Chem.* **1996**, *100*, 7911-7918. Herzberg, G.; Johns, J. W. C. *J. Chem. Phys.* **1971**, *54*, 2276. Jensen, P.; Bunker, P. R. *J. Chem. Phys.* **1988**, *89*, 1327. Duxbury, G.; Jungen, Ch. *Mol. Phys.* **1988**, *63*, 981. Petek, H.; Nesbitt, D. J.; Darwin, D. C.; Ogilby, P. R.; Moore, C. B.; Ramsay, D. A. *J. Chem. Phys.* **1989**, *91*, 6566.

(27) We thank a reviewer for this suggestion.

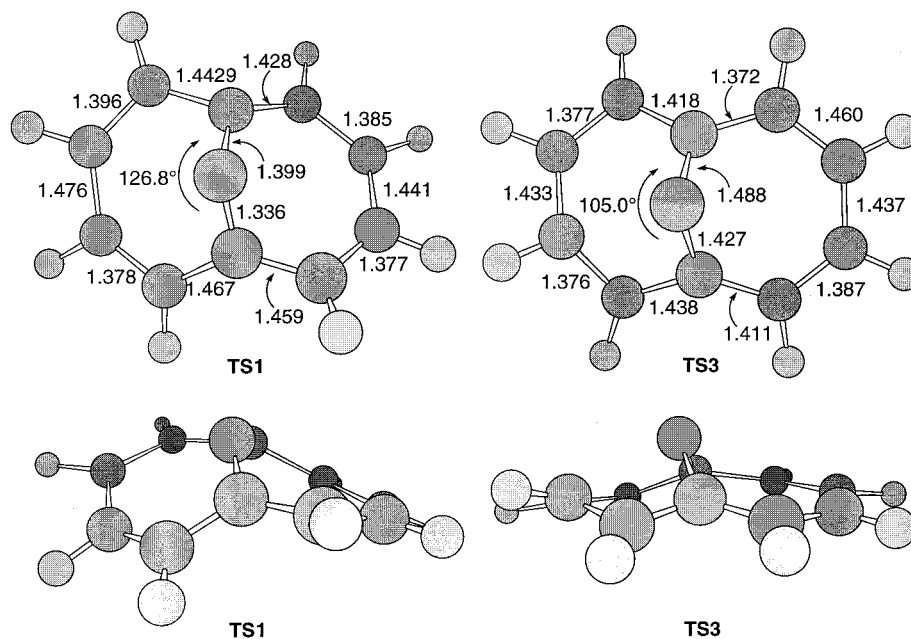


Figure 6. Bond lengths and $C_1-C_{11}-C_6$ bond angles for transition states **TS1** and **TS3** (top, view from top; bottom, side perspective). The values given were calculated at the B3LYP/6-31G(d) level; bond lengths are given in angstroms and are indicated in the figure by full arrows; bond angles are indicated using half-arrows.

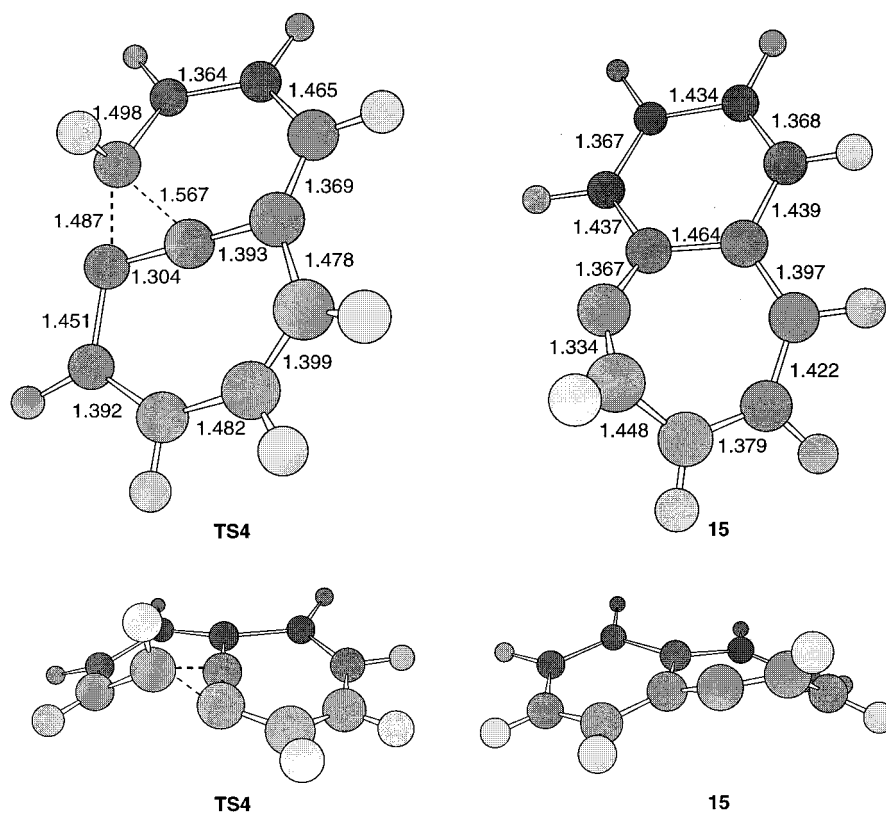


Figure 7. Bond lengths and selected bond angles for transition state **TS4** and **15**. The values given were calculated at the B3LYP/6-31G(d) level; bond lengths are given in angstroms.

formation of **8**), which then undergoes intermolecular trapping with DPIBF, and occurs prior to the high-energy rearrangement to more stable isomers such as **15**.

Is 5 Aromatic? The parent compound of **5S**, 1,6-methano[10]annulene, was shown to be aromatic some years ago.⁹ Part of the inspiration for the original work on that molecule was to test whether a molecule with a nonplanar π system could maintain aromaticity, despite

the disruption in π overlap. A plethora of physical and computational investigations⁹ have definitively shown that, although the methano bridge forces a departure from planarity in the 10-membered ring, 1,6-methano[10]annulene is indeed aromatic. In an effort to assess the potential changes in aromaticity upon replacement of the methylene group in the parent annulene with a carbenic carbon, we analyzed both **5S** and the parent

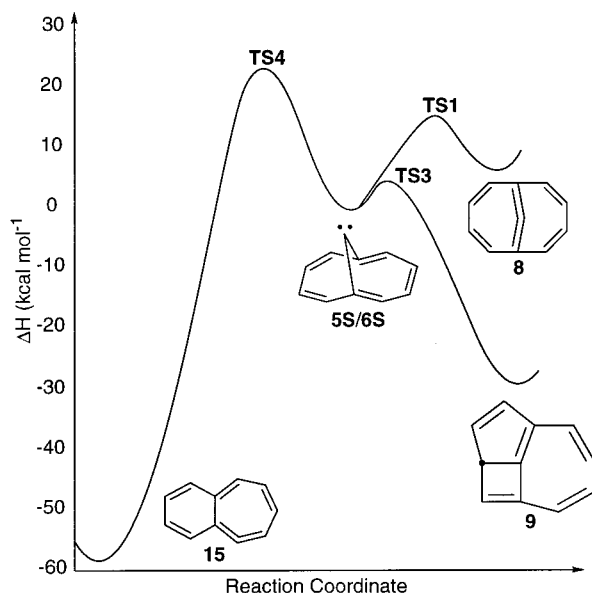


Figure 8. PES for the rearrangement of carbene **5**. All energies are reported at the B3LYP/TZP//B3LYP/6-31G(d) level.

annulene using three different criteria: (a) bond distance changes in the 10-membered ring, (b) examination of the molecular orbitals, and (c) shifts in the hydrogen and carbon magnetic shielding tensors.

Calculations at the B3LYP/6-31G(d) level indicate that the bond distances within the 10-membered ring in **5S** and the parent annulene do not vary appreciably (i.e., $<0.006 \text{ \AA}$). The most notable change in the bond length occurs between the carbene carbon (C_{11})/methano group and the adjacent bridgehead carbons C_1 and C_6 , for which we find distances of 1.458 and 1.493 \AA , respectively. These values indicate a slightly more pronounced interaction between the carbene carbon and the 10-membered ring than that which exists in the parent annulene. As we pointed out in the Spin-State section, examination of the molecular orbitals provides an indication of the ability of the carbene carbon to interact with the 10-membered ring. The only carbene orbitals that are of the correct symmetry to interact with the aromatic ring are high-energy unoccupied orbitals (interacting with the occupied carbene σ orbital) and low-energy occupied orbitals (interacting with the unoccupied carbene p orbital). These interactions are not energetically matched and indicate little participation with the π system of the 10-membered ring. Analysis of the molecular orbitals indicates a slightly more pronounced σ -bonding interaction for **5S** between the carbene carbon and C_1 and C_6 , which is consistent with an increase in sp^2 character in the carbene carbon and the corresponding decrease in bond length. No other differences exist in the bonding π orbitals of the 10-membered ring. Thus, according to these criteria, we find very little difference between **5S** and the parent annulene in terms of changes in the overall aromaticity of the 10-membered ring upon replacement of the methano group with a carbenic center.

The final comparison involved comparison of the magnetic shielding tensors calculated at the HF/6-311+G-(2d,p)//B3LYP/6-31G(d) level for both **5S** and the parent annulene. This computational level gives good agreement with the experimentally determined ^1H and ^{13}C NMR

shift values for the parent annulene.²⁸ Comparison of the calculated shielding tensors for **5S** and the parent annulene yields only minor changes (~ 1 ppm) in the hydrogen tensors but more variable changes in the carbon tensors.²⁸ Changes in the hydrogen atom tensors are not expected to be large even if the aromaticity is disturbed, because aromatic hydrogens typically absorb $\sim 7\text{--}8$ ppm, and olefinic hydrogens, $\sim 5\text{--}6$ ppm. A more noticeable difference, however, occurs at the carbon atoms, particularly those atoms adjacent to the bridging positions (i.e., C_2 , and symmetry-related positions on the ring) for which an ~ 36 ppm upfield shift is observed for **5S** relative to the parent annulene. The bridgehead carbons (C_1 and C_6) shift downfield by ~ 21 ppm, while the remaining carbon atoms in the 10-membered ring shift ~ 2 ppm downfield. Localized changes in the shielding tensors (i.e., C_1 , C_6 , and the C_2 -related carbons) are to be expected, given the change in electronegativity at the carbene carbon because of the removal of the two hydrogen atoms from the methano bridge, and thus shifts at these positions are not surprising. More important are the negligible changes in the magnitudes of the shielding tensors for the carbon atoms once removed from the bridging carbons (i.e., C_3 , C_4 , C_8 , and C_9), which incur only an ~ 2 ppm downfield shift. If the aromaticity of **5S** were substantially perturbed, a much larger change would be expected for these carbons. We do not therefore believe that the shift tensors indicate any tendencies toward a break in aromaticity in **5S**. In conclusion, the data we have considered are all consistent with little change in the predicted aromaticity of **5S**, and we believe there is little reason to suspect a disruption in the aromatic character of the annulene ring resulting from the replacement of the methylene group in 1,6-methano-[10]annulene with a carbene carbon.

In conclusion, the initially formed carbene, **5S/6S**, rapidly rearranges to form the closed-shell, tricyclic product **9**. This kinetically favored reaction channel (**5** \rightarrow **9**) is followed because of a low energetic barrier ($\Delta H^\ddagger \sim 5.1 \text{ kcal mol}^{-1}$). Reactions through transition states **TS1** ($\Delta H^\ddagger \sim 16.5 \text{ kcal mol}^{-1}$) and **TS4** ($\Delta H^\ddagger \sim 23.1 \text{ kcal mol}^{-1}$), yielding as products **8** and **15**, respectively, are not observed because of higher activation energy barriers. Thus, it appears the intermediate trapped by Levin was **9**, which is more stable than **8** by $\sim 35 \text{ kcal mol}^{-1}$.

Acknowledgment. The author thanks Professor David Perry (The University of Akron) for a fruitful discussion and Dr. Allan East (The University of Akron), Professor Al Matlin (Oberlin College), and Professor Paul M. Lahti (University of Massachusetts, Amherst) for helpful comments on the manuscript.

Supporting Information Available: Energies and Cartesian coordinates for **5–10**; **15**; and **TS1**, **TS3**, and **TS4**. This material is available free of charge via the Internet at <http://pubs.acs.org>.

JO000181N

(28) Experimental value (ppm, referenced to TMS; calculated value in parentheses): $C_1=C_6 = 115.0$ (115.6); $C_2=C_5=C_7=C_{10} = 126.2$ (132.2); $C_3=C_4=C_8=C_9 = 128.8$ (130.0); $C_{11} = 24.9$ (27.9). Modarelli, D. A. Unpublished data. ^{13}C NMR values are found in the following: Günther, H.; Schmickler, H.; Königshofen, H.; Recker, K.; Vogel, E. *Angew. Chem.* **1973**, *85*, 261. ^1H NMR values are found in the following: Vogel, E. *Aromaticity. Chem. Soc. Spec. Publ.* **1967**, *21*, 113.